JOURNAL OF SOLID STATE CHEMISTRY 100, 281–291 (1992)

# Evidence for Nickel-(I)-Rich Mixed Oxide with a Defect $K_2NiF_4$-Type Structure

M. CRESPIN,* C. LANDRON,† P. ODIER,† J. M. BASSAT,† P. MOURON,‡ AND J. CHOISNET‡

*Centre de Recherche sur la Matière Divisée, CNRS 45071 Orléans Cedex 2, France; ‡Centre de Recherche sur la Matière Divisée, Université d'Orléans, 45067 Orléans Cedex, France; and †Centre de Recherche sur la Physique des Hautes Températures, CNRS 45071 Orléans Cedex 2, France

Received November 20, 1991; in revised form March 19, 1992; accepted March 26, 1992

Reduced phases obtained from lanthanum mixed nickel oxide, i.e., $La_{2-x}Sr_xNiO_{4-y}$, $K_2NiF_4$ type, have been studied. Reduction under controlled conditions led to the composition $LaSrNiO_{3.1}$ containing formally more than 80% of Ni in the valence state (I). Structural calculations and local studies by X-ray adsorption spectroscopy provide evidence for a lowering of the Ni octahedral coordination configuration. V-square-pyramidal and IV-square configurations are obtained, depending on the reduction level. The oxygen vacancies are highly ordered along the *b* axis of the orthorhombic unit cell, in agreement with recent defect modeling of this structure 

## Introduction

Lanthanum nickelate $La_2NiO_{4+\delta}$ ($\delta \geq 0$) and strontium-substituted phases $La_{2-x}Sr_xNiO_y$ are in many aspects of their crystal chemistry strongly related to the corresponding cuprates, especially those of composition $La_{2-x}Sr_xCuO_4$ which exhibit high $T_c$ superconductivity (*2*). Taking into account the role played by the $d^9$ copper electronic configuration in crystal chemistry and physical properties of these cuprates, one must consider the possible existence of such a $d^9$ configuration in the nickelate family. The usual valence state of Ni is (II), with a $d^8$ configuration; hence, only reducing conditions should be able to induce the Ni (I) state in these mixed oxides. In fact, such phases have already been reported in La–Ni–O and La–Sr–Ni–O systems. One of us (M.C.) prepared and studied the reduced perovskite $LaNiO_2$ (*3*); later, the strongly oxygen-deficient compound $La_{1.6}Sr_{0.4}NiO_{3.47}$ (*4*) was synthesized and structurally characterized as a defect-ordered $K_2NiF_4$ structure. A similar procedure, i.e., progressive reduction by hydrogen at low temperature ($T <$ 700 K), was recently applied to cuprates belonging either to the T phase ($K_2NiF_4$) or to the T′ phase ($Nd_2CuO_4$) (*5*).

In this paper, we report on new results regarding the reduced nickelates $La_{2-x}Sr_xNiO_y$ ($0 \leq x \leq 1$) with the ordered defect $K_2NiF_4$-type structure. As an example, $LaSrNiO_{3.1}$ has been obtained, containing as much as 80% of nominally Ni (I). Both the crystallographic characterization and the analysis of the local Ni environment by EXAFS and XANES provide evidence for a low (I) valence state of Ni. We compare



0022-4596/92 $5.00

the crystal chemistry of reduced nickelates with that of both their fully oxidized parent phases and corresponding cuprates. In addition, conclusions concerning favorable sites for oxygen vacancies in $La_{2-x}Sr_xMO_y$ ($M$ = Ni, Cu) are drawn for nickelates and extrapolated to cuprates, thus addressing a problem that could be related to the lowering of $T_c$ above $x = 0.15$.

## Experimental

### *Sample Preparation*

The samples $La_{2-x}Sr_xNiO_y$ are initially prepared in their oxidized state by solid-state reaction in air at high temperature. The precursor powder is obtained by a solution polyacrylamide-gel route (*6*), which efficiently produces ultrafine powders with a high chemical homogeneity, even for complex compositions. After drying the gel, the powder is calcined at increasing temperature up to 1420 K and slowly air-cooled (100 K/hr) to room temperature. This procedure yields a very reactive black powder with a high oxygen content, which was checked to be monophasic by X-ray diffraction. $LaSrNiO_{4.0}$ has been prepared by this procedure, its oxygen content being determined by weight loss measurements in a total reduction under Ar-5%$H_2$ in a thermal-gravimetric apparatus. We stress that sintering and annealing in air at 1520 K, followed by a fast cooling (>500 K/hr) give rise to a slightly lower oxygen content, i.e., $LaSrNiO_{3.8}$.

The same experimental setup for the controlled reduction as for preparing $LaNiO_2$ (*4*) was used, i.e., a heated all-glass vessel in which a measured amount of pure hydrogen was circulated by a magnetically activated pump (Fig. 1). Before any experiment, the sample and the apparatus were submitted to a cleaning procedure: overnight heating at 900 K under oxygen to eliminate all traces of organic residues, followed by purging of the system for a few minutes in vacuum. The system is then cooled down and a total reduction at 900 K is performed to determine the oxygen content in the oxidized state. This is done on a part of each sample. A slow partial reduction is performed at moderate constant temperature ($T \leq 670$ K) in order to form phases containing Ni (I). The volumetric measurement of $H_2$ consumption (oxygen evolved) is performed versus time until no significant evolution of the evolved oxygen is detected after at least 10 hr. In such a case the experiment is stopped, then the sample is quenched and stored in an evacuated desiccator. However, no significant changes in the samples are observed when storing in air. Combining the results of both the total and the partial reduction one can calculate the oxygen content of the reduced nickelates; it is plotted in the curves of Fig. 2. The total reduction step has been compared to the weight loss measured in the TGA runs. Both measurements agree to better than 2% in the measured oxygen content.

### *X-ray Diffraction (XRD)*

XRD was used first to characterize the parameters of the unit cell and to perform structure calculations. Powder diffractograms were recorded from a Siemens D 500 apparatus by using Cu$K\alpha$ radiation. A least-squares refinement procedure based upon the integrated intensities of diffraction peaks provides a check on the reliability of the structural model, i.e., an ordered oxygen-deficient $K_2NiF_4$-type structure.

### *EXAFS and XANES*

An analysis of the local site configuration of nickel was undertaken by studying both the oxidation state using XANES and the coordination and bond length using EXAFS. This study was performed for several compositions of oxidized and reduced nickelates for purposes of comparison. Seven different compositions of nickelates were thus studied. The samples were sepa-

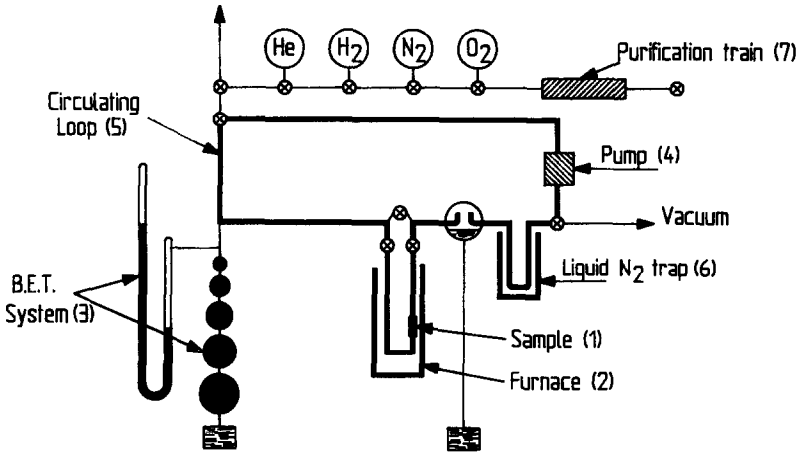


FIG. 1. Experimental set up for controlled reduction of oxides. (1) Sample, (2) furnace, (3) gas burette with a mercury manometer, (4) magnetic pump activating the circulating loop (5). The gas passes through a liquid nitrogen trap (6). Storing ring for gas (He, $H_2$, $N_2$, $O_2$) with a purification train (7). The system can be evacuated using a vacuum pump.

rately ground to obtain micrometer-sized powders and then pressed onto kapton tapes. The XAS measurements were carried out in a transmission mode at LURE (Orsay) at the Ni *K*-edge (8320–8430 eV energy range for XANES and 8200–9300 eV energy range for EXAFS data). Synchrotron radiation was provided by the 1.85 GeV storage ring of DCI, the experiments being done in ambient air. The X-ray beam of the EXAFS III station was monochromatized by a double reflection (311) on an Si crystal. The intensity of the positron beam was about 300 mA. We used air-filled ionization chambers to measure the photon intensity in front of and behind the target.

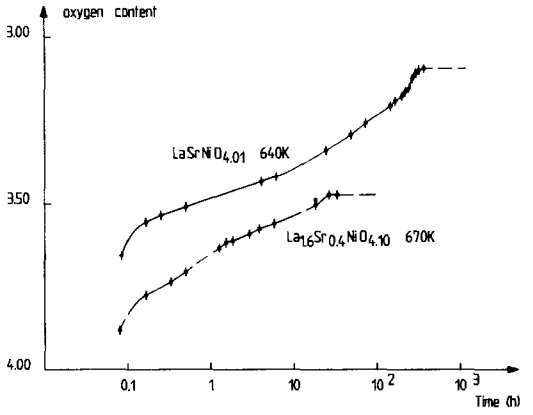


FIG. 2. Oxygen content versus time in partial reduction of $La_{1.6}Sr_{0.4}NiO_{4.1}$ (a), and $LaSrNiO_{4.0}$ (b). The $H_2$ volume consumed by the reduction is plotted on the right scale.

## Results

### *Reduced Mixed Nickelates*

The above reduction procedure yields the mean oxidation state and may serve to detect phases. As an example, starting from an oxidized phase, one observes a fast preliminary elimination of oxygen which is followed by a first plateau, as proved by the abrupt change of the slope (Fig. 2); this plateau is more or less defined according to the temperature of reduction. These oxides are yellow-brownish powders, their corresponding oxygen stoichiometry fits rather well the formula $La_{2-x}Sr_xNiO_{4-x/2}$. Consequently, they are assumed to be pure Ni(II)

phases. Undoped lanthanum nickelate ($x$ = 0) gives a composition that under the actual measurement precision is probably $La_2NiO_4$, a brown-colored orthorhombic phase ($a$ = 5.468 Å, $b$ = 5.539 Å, $c$ = 12.56 Å). It is similar to that formed by Saez-Puche and others (*7, 8*). EXAFS and XANES results on this phase are presented below. Attempts to reduce more this phase led to its decomposition in $La_2O_3$ + Ni.

A further increase of the reduction level can be reached for the mixed lanthanum strontium nickelates, $La_{2-x}Sr_xNiO_y$. The oxygen content is decreased down to approximately 3.5, i.e., $La_{1.6}Sr_{0.4}NiO_{3.5}$, and 3.1, i.e., $LaSrNiO_{3.1}$, respectively, for $x$ = 0.4 and 1. This is evidenced by the existence of a well defined second plateau (Fig. 2). $LaSrNiO_{3.5}$ has been formed in the same manner by carefully controlling the $H_2$ consumption and interrupting the experiment at the appropriate oxygen stoichiometry. The influence of strontium is clearly proved by our inability to achieve a reduction of $La_2NiO_4$. Such a procedure only results in triggering the destruction of $La_2NiO_4$.

At this stage, we emphasize the similarities in behavior of $La_{2-x}Sr_xNiO_y$ oxides with respect to both oxidation or reduction. As demonstrated by others (*9–11*), increasing the Sr content to $x$ = 1 increases the valence of the nickel to the Ni (III) oxidized state. Conversely, by de-oxygenating under hydrogen, the theoretical lower limit for oxygen stoichiometry ($O_3$) is also nearly attained for $x$ = 1, our own results pointing to the composition $O_{3.1}$, i.e., to a conversion of 80% of the total nickel into the Ni(I) valence state.

*Crystallographic Characterization*

The $LaSrNiO_y$ ($y$ = 3.5, 3.1) family is now discussed from the crystallographic point of view, as an interesting example which exhibits a variation in Ni (I) content from 0% to 80%.

The reduced nickelates $LaSrNi(II)O_{3.5}$ and $LaSrNi(I,II)O_{3.1}$ were characterized by using X-ray powder diffractograms recorded up to $2\theta$ = 100°. As previously found for $La_{1.6}Sr_{0.4}NiO_{3.47}$ (*4*) the unit cell is orthorhombic with $a \simeq b = a_p$ (the parameters of the primitive perovskite unit cell). Table I reports the values of $a$, $b$, $c$, and of the unit cell volume, together with those of the oxidized phase $LaSrNiO_4$ (*11, 9*). Clearly, the orthorhombicity of the unit cell increases with increasing reduction: $a/b$ = 1.04 for "$O_{3.5}$" as compared to 1.08 for "$O_{3.1}$." However, the unit cell volume remains almost constant from "$O_4$" (Ni(III)) to "$O_{3.5}$" (Ni(II)) and then decreases for the fully reduced composition "$O_{3.1}$" (Ni(I)). The increase in the $c$ parameter upon reduction is more than balanced by the significant shrinkage of the b parameter.

TABLE I

LATTICE PARAMETERS (Å) OF $LaSrNiO_y$ PHASES, $y$ = 4, 3.5, 3.1

| $y$ | 4[10] | 3.5 | 3.1 |
|---|---|---|---|
| $a$ | 3.826(5) | 3.8666(6) | 3.853(2) |
| $b$ | 3.826(5) | 3.7281(9) | 3.566(3) |
| $c$ | 12.45(2) | 12.644(1) | 12.869(11) |
| $V$(Å$^3$) | 182.25 | 182.26 | 176.82 |

*Note.* Standard deviations are in brackets.

*Structure Calculates*

Structure calculations were carried out from the integrated intensities of X-ray powder diffractograms: in the range $5° \leq 2\theta \leq 100°$, 49 *hkl*(47), i.e., 32 intensities (31) for $LaNiO_{3.5}$ and $LaSrNiO_{3.1}$, respectively, were used in a least-squares refinement procedure of the variable parameters. The only limiting condition on (*hkl*), $h + k + l = 2n$, is consistent with the choice of the space groupe *Immm* in the orthorhombic system as previously done for $La_{1.6}Sr_{0.4}NiO_{3.47}$ (*4*), $Sr_2CuO_3$ (*12, 13*), and $Ba_2CuO_{3.3}$ (*14*). The refinement procedure includes the atomic

TABLE II

ATOMIC PARAMETERS OF THE DEFECT $K_2NiF_4$-TYPE STRUCTURE OF ($\alpha$) $LaSrNiO_{3.5}$ AND ($\beta$) $LaSrNiO_{3.1}$

| Atom | Position | $x$ | $y$ | $z$ | $B$(Å$^2$) | Site occupancy |
|---|---|---|---|---|---|---|
| La, Sr | 4($i$) | 0 | 0 | $\alpha$0.3586(2) | 1.2(1) | 1.0[a] |
| | | | | $\beta$0.3587(2) | 1.0(1) | 1.0[a] |
| Ni | 2($a$) | 0 | 0 | $\alpha$ 0 | 1.5(1) | 1.0[a] |
| | | | | $\beta$ 0 | 2.7(2) | 1.0[a] |
| O(1) | 4($i$) | 0 | 0 | $\alpha$0.164 (1) | 1.1(1) | 1.0[a] |
| | | | | $\beta$0.159 (1) | 0.6(1) | 1.0[a] |
| O′(2) | 2($b$) | 0.5 | 0 | $\alpha$ 0 | 1.5(1) | 1.00(2) |
| | | | | $\beta$ 0 | 1.1(1) | 0.89(2) |
| O″(2) | 2($d$) | 0 | 0.5 | $\alpha$ 0 | 1.5(1) | 0.43(2) |
| | | | | $\beta$ 0 | 0.6(1) | 0.20(2) |

*Note.* RI($\alpha$) = 0.036; RI($\beta$) = 0.058.
[a] Not refined.

parameters—$z$ values for (La, Sr) and axial $O_{(2)}$ oxygen, isotropic thermal factors of all the atoms—and the occupancy factors of the two sets of equatorial oxygen: $O'_{(2)}$ (position 2$b$) and $O''_{(2)}$ (position 2$d$). Table II reports the values obtained after refinement: the RI confidence factor vs intensities is respectively equal to 0.036 for $LaSrNiO_{3.5}$ and 0.058 for $LaSrNiO_{3.1}$; Fig. 3 gives a schematic representation of the structure.

Although not so accurate as those deduced from the Rietveld profile analysis, the results herein obtained point to significant trends of the oxygen nonstoichiometry and related ordering phenomena. In this respect, the amount of oxygen defect is large enough to be recorded in a satisfying way. As a proof—see Table II—the calculated value of the total amount of oxygen which is located in the $O'_{(2)}$ and $O''_{(2)}$ sites of the equatorial "$NiO_2$" plane, $-2.86$ for $LaSrNiO_{3.5}$ and 2.18 for $LaSrNiO_{3.1}$, slightly deviates from the chemical value $-3$ and 2.20 respectively. More precisely, the location of the oxygen vacancies is strongly ordered in the equatorial planes, along the $b$ axis. Other distributions of oxygen vacancies, e.g., either statistical or ordered along the a axis, give rise to a significantly higher $R_I$ factor ~0.1 accompanied by unrealistic values of thermal factors at oxygen positions that become either very large, $\geq 5$ Å$^2$ or negative. The thermal factor at the Ni position has a rather high value in the case of $LaSrNiO_{3.1}$, i.e., 2.7 (Å$^2$), see Table II. A similar value, 2.4 (Å$^2$), was previously obtained for Ni in the reduced nickelate $La_{1.6}Sr_{0.4}NiO_{3.5}$ (*4*). It is in fact smaller that the same factor for copper ($B$(Cu) = 3.1 (Å$^2$)) reported by D. M. de Leeuw *et al.* (*14*) for the deficient $Ba_2CuO_{3.3}$, which exhibits nearly the same ordered lacunar structure as these nickelates. Obviously, this cannot be held as an

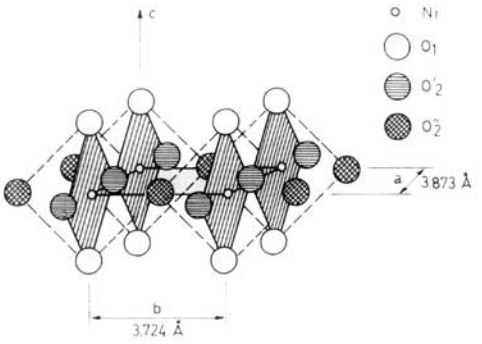


FIG. 3. Structure of the reduced mixed nickelates "$O_{3.1}$." Oxygen vacancies are highly ordered in the $b$ direction: $O''_2$ site occupancy is only 20%.

TABLE III

MAIN INTERATOMIC DISTANCES (Å) IN THE MIXED NICKELATE $LaSrNiO_y$ ($y$ = 4, 3.5, AND 3.1) IN THREE OXIDATION STATES: III, II, AND I

| | "$O_4$" [10] | "$O_{3.5}$" | "$O_{3.1}$" |
|---|---|---|---|
| Ni–$O_2$ | 4 × 1.91 | $O'_2$ **2 × 1.93** (70%) | $O'_2$ **2 × 1.93** (81%) |
| equatorial | | $O''_2$ 2 × 1.86 (30%) | $O''_2$ 2 × 1.78 (19%) |
| Ni–$O_1$ | 2. × 2.05 | 2 × 2.07 (1) | 2 × 2.04 (1) |
| axial | $\sigma$ = 0.14 | $\sigma$ = 0.14 | $\sigma$ = 0.11 |
| La, Sr–$O_1$ axial | 1 × 2.44 | 1 × 2.47(2) | 1 × 2.58 (2) |
| equatorial | 4 × 2.72 | 4 × 2.70 | 4 × 2.63 |
| La, Sr–$O_2$ | 4 × 2.58 | $O'_2$ **2 × 2.63(1)** | $O'_2$ **2 × 2.65 (1)** |
| | | $O''_2$ 2 × 2.58 (1) | $O''_2$ 2 × 2.65 (1) |
| | $\sigma$ = 0.28 | $\sigma$ = 0.23 | $\sigma$ = 0.07 |

*Note.* $\sigma$ is the largest cation–O distance deviation in the "octahedron" and in the (La, Sr) coordination polyhedron. Boldface indicates the most probable distance.

answer for the occurrence of such a high value; nevertheless, the reason is to be found in the strong oxygen deficiency of the "$NiO_2$" planes, possibly resulting in an anisotropic thermal motion of the cations toward the $O''_{(2)}$ site.

Of special interest are the results concerning $LaSrNiO_{3.1}$. The level of reduction is close to the maximum which can be expected, and the structural data are in many respects close to that of $K_2NiF_4$-type structure corresponding to $Sr_2CuO_3$ (*12, 13*). As a striking feature, the IV-square coordination of Ni(I) atoms, which is the limiting one for the hypothetical composition "$LaSrNiO_3$", ensures the very similar behavior of Ni(I) in this phase and Cu(II) in $Sr_2CuO_3$.

The main interatomic distances for $LaSrNiO_{3.5}$ and $LaSrNiO_{3.1}$ are reported in Table III, together with those of the fully oxidized phase $LaSrNiO_4$ (*11, 9*). In a statistical sense, the most probable coordination of Ni is fivefold in $LaSrNiO_{3.5}$ and fourfold in $LaSrNiO_{3.1}$. Regarding the equatorial Ni–O distances, the most probable one (Ni–$O'_2$) is rather insensitive to the level of reduction. The same trend is observed for the axial: Ni–$O_1$ distances. Therefore, the distortion of the Ni environment (as measured by $\sigma$, see Table III) does not change very much with the reduction level that is achieved by decreasing the nickel valency from (III) to (I).

Conversely, the largest effect of the reduction process is found in the coordination polyhedron of La (strontium) atoms. The so-called ninefold coordination polyhedron of the $K_2NiF_4$ structure is progressively turned in a seven-fold limiting one, as observed for the cuprate $Sr_2CuO_3$. Moreover, this polyhedron gets more and more symmetrical as the Ni(I) content increases, 4 × 2.70 Å + 1 × 2.47 Å in "$O_{3.5}$" and 4 × 2.63 Å + 1 × 2.58 Å in "$O_{3.1}$" for the La(Sr)–O axial bond, see Table III. It is worthwhile to emphasize the behavior of this axial La(Sr)–O bond. The strain, i.e., the compression which exists in the structure of "$O_4$" stoichiometric compound, on the La–O axial bond is relaxed by decreasing the effective charge in the perovskite layer and in the $AO$ NaCl-type layer. As a consequence, the

2D character of the structure is greatly lowered in the reduced phase.

*Local Structure: XANES and EXAFS*

The above structural model of the mixed reduced nickelates $LaSrNiO_y$ was tested by directly probing the local environment of the nickel site using XAS experiments. Both XANES and EXAFS results are reported below. A complete mathematical treatment is needed to reduce the raw data to normalized data for EXAFS analysis. The structural informations were derived from the calculation of the interference between the outgoing and the backscattered wave. The mathematical treatment of the spectra is based on the procedure previously described (*15*) and will also be detailed elsewhere. The data were first calibrated, averaged and normalized. The background was subtracted and the EXAFS oscillations were Fourier transformed. The *k*-space used for the Fourier transform was limited by $k_{min} = 26\ nm^{-1}$ and $k_{max} = 120\ nm^{-1}$. The least-squares fitting method for coordination shell determination has been employed with the values of phases and amplitudes calculated according to the procedure of McKale *et al.* (*16*). The free parameters used in the fit procedure were the interatomic Ni–O distances, the coordination numbers, the *K*-edge positions, and the Debye–Waller factors; the mean free path was chosen identical for all the studied compounds (see Table IV). It was calculated from refined data of $La_2NiO_{4+\delta}$ the structure of which is known (*17, 18*). The reliability factors of least square fitting of the data were similar for the various samples and they were satisfactory.

*XANES.* We have compared oxidized nickelates (as prepared): $La_2NiO_{4+\delta}$ ($\delta$ = 0.16), $La_{2-x}Sr_xNi_{4+\delta}$, (respectively $x = 0.4$, $\delta = 0.1$; and $x = 1$, $\delta = 0.0$) with reduced nickelates: $La_{2-x}Sr_xNiO_y$ (respectively $x$ = 0.4, $y = 3.47$; and $x = 1$, $y = 3.1$). The spectra of oxidized compounds are identical and cannot be distinguished; therefore, only that of $La_2NiO_{4+\delta}$ has been plotted and compared with the reduced Sr-substituted nickelates in Fig. 4. "$O_4$" and "$O_{3.5}$" are similar, but shifted with respect to each other on the energy scale. The spectrum for "O3.1" appears with a slightly different shape with new structure at low energy. The shift to the lower energy is due to the decrease in the screening potential of Ni in the reduced valency state. It is estimated from the position of the main peak and reaches 3 eV between $La_2NiO_{4.16}$ (spectrum a) and $La_{1.6}Sr_{0.4}NiO_{3.5}$ (b), in agreement with a decrease in the "mean valency" of the Ni as already reported for reduced $LaNiO_3$ (*3*). It may be argued that these reduced phases might contain nickel in the Ni (0) state, but present in amounts too small to be detected by XRD. By comparison, a totally reduced lanthanum nickelate has been measured Fig. 4d. The spectrum for this sample is quite similar to that of a nickel metal foil also investigated in this run: Fig 4e. Spectrum (d) is quite different from (a), (b), and (c), and is very likely characteristic of Ni (0) metal atoms (clusters) with a low coordination number (*19*). M. Hida *et al.* (*20*) and T. Bein *et al.* (*21*) have reported similar conclusions concerning EXAFS investigation of Ni fine particles prepared by gas evaporation or thermal decomposition of supported $Ni(CO)_4$ as a precursor for dispersed Ni-cluster catalysts in zeolite. We confirm the complete reduction of the nickelates in Fig. 4d from the fact that the Fourier transform exhibits only one peak corresponding to an Ni–Ni bond without any contribution occurring at the Ni–O bond length. This provides evidence for the formation of small clusters of Ni dispersed in lanthanum oxide. Moreover, the low-temperature magnetism for sample "$O_{3.5}$" or "$O_{3.1}$" (Figs. 4b and 4c) does not display any large ferromagnetism component, as would occur if several percent of nickel were in the Ni(0) state (*22*).

*EXAFS.* We have used the standard math-

TABLE IV

Ni–O Bond Lengths (Å) and Ni Coordination Numbers Obtained by Simulation of EXAFS Spectra for Several $La_{2-x}Sr_xNiO_y$ Phases in Both Reduced and Oxidized States

| Sample | $La_2NiO_{4.16}$ | $La_2NiO_{3.95}$ | $La_{1.6}Sr_{0.4}NiO_{4.1}$ | $La_{1.6}Sr_{0.4}NiO_{3.5}$ | $LaSrNiO_4$ | $LaSrNiO_{3.1}$ |
|---|---|---|---|---|---|---|
| Subshell 1 | | | | | | |
| Ni–O Dist. | 1.94(2) | 1.95(2) | 1.91(2) | 1.90(2) | 1.91(2) | 1.90(2) |
| Coord. numb. | IV | IV | IV | III | IV | 2.5 |
| Subshell 2 | | | | | | |
| Ni–O Dist. | 2.21(2) | 2.24(2) | 2.13(2) | 2.21(2) | 2.09(2) | 2.03(2) |
| Coord. numb. | II | II | II | II | II | II |

*Note.* Distances are in Angstroms. The precision on the coordination numbers is 15%. The fractional coordination number 2.5 + 2 indicates a statistical distribution of both fourfold and fivefold coordinations. Debye–Waller factors are 0.07 Å ± 0.005 for sub-shell 1 and 0.08 Å ± 0.005 for sub-shell 2.

ematical technique to fit the experimental data for which the EXAFS signal above the Ni edge has been analyzed in terms of the known theory of X-ray absorption developed by Teo (*23*). As an example, Fig. 5gives the modulus (full line) and the imaginary part (dotted line) of the Fourier transform corresponding to the $k^3$-weighted EXAFS spectrum of (a) $La_{1.6}Sr_{.4}NiO_{4.1}$ and (b) $La_{1.6}Sr_{.4}NiO_{3.5}$ samples, recorded for the Ni *K*-edge. Simulations of the EXAFS spectra provide quantitative information concerning the Ni–O bond lengths for the first and second shell and the Ni coordination numbers in the various samples for both oxidized or reduced phases. The results are reported in Table IV.

From the number of first and second neighbors observed for the oxidized phases, one clearly observes the usual (IV + II) distortion of the $NiO_6$ octahedron. The rather weak reduction of the undoped lanthanum nickelate, i.e., $O_{4.16} \rightarrow O_4$, does not modify the coordination number of Ni, whereas for the lanthanun strontium phase the strong reduction, i.e., $O_{4.10} \rightarrow O_{3.5}$, results in a lowering of the coordination from VI to V and even to IV in the most reduced compound $LaSrNiO_{3.1}$. This trend is in perfect agreement with the result of X-ray

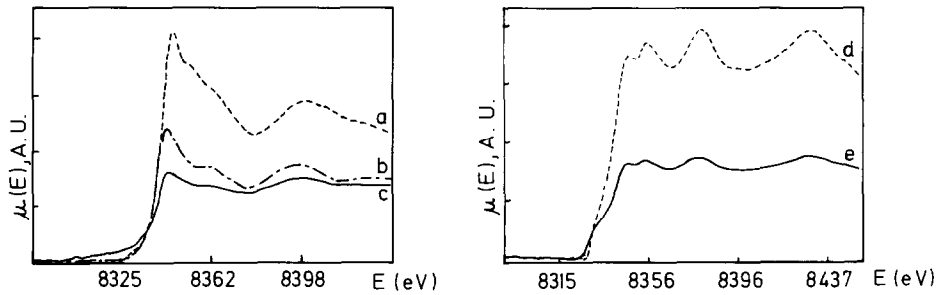


FIG. 4. X-ray absorption near nickel *K*-edge structure (XANES) of mixed nickelates for different oxidation state. Ordinate: the adsorption coefficient (arbitrary unit); abscissa: the energy in eV. The curves of the left hand part correspond to (a) $La_2NiO_{4+\delta}$; (b) $La_{1.6}Sr_{.4}NiO_{3.5}$; and (c) $LaSrNiO_{3.1}$. On the right hand part we compare (d) totally reduced lanthanum nickelate and (e) pure nickel foil.

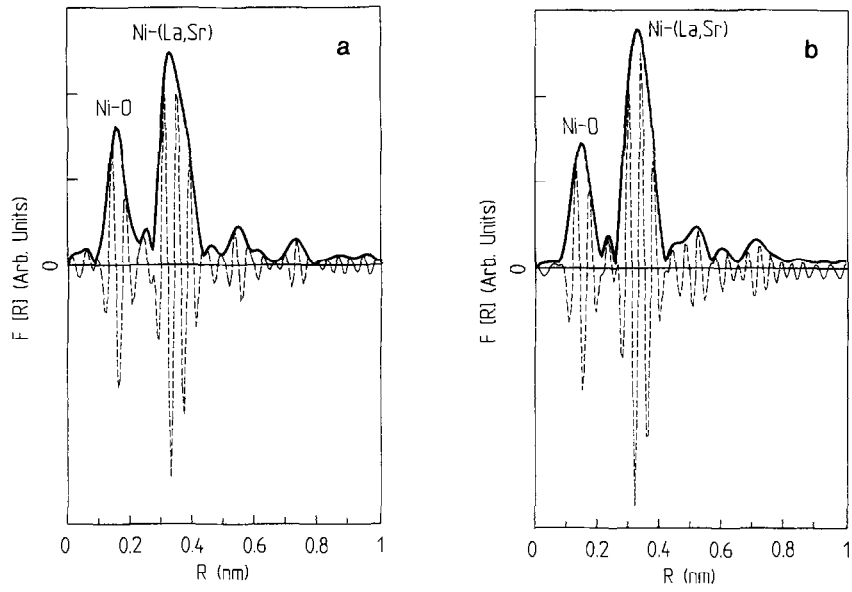


FIG. 5. Modulus (full line) and imaginary part (dotted line) of the Fourier transform corresponding to the $k^3$-weighted EXAFS spectrum of $La_{1.6}Sr_{0.4}NiO_4$ (a) and $La_{1.6}Sr_{0.4}NiO_{3.5}$ (b). The pseudo-radial distribution functions are uncorrected for the phase shift of the Ni–O and Ni–(La, Sr) pairs.

structural study. At the same time, no significant modification of the in-plane Ni–O distances (subshell 1) is observed; the axial Ni–O distance (subshell 2) is more affected in the reduction process.

## Discussion

A striking result of this study is the excellent agreement between the X-ray structural modelling of the local arrangement around the Ni atoms and the corresponding EXAFS and XANES results. Upon decreasing the number of oxygen atoms, the structure is continuously modified but without the formation of new structures; on the contrary, the parent structure is likely to be preserved. The new arrangement only involves movements of atoms over short distances. This is another example of the extended tolerance for nonstoichiometry which characterizes the perovskite structure.

Removing oxygen from the $La_{2-x}Sr_xNiO_y$ involves essentially the *a-b* plane "$NiO_2$," as is seen from either structural calculation or local characterizations. Both lead to oxygen vacancies ordering along the *b* direction (Table II), which is consistent with a systematic lowering in the number of oxygen neighbors of Ni (Table IV). In the most reduced phase, i.e., $LaSrNiO_{3.1}$, the nickel atoms appear to be coordinated by four oxygens, in a distorted square. Note that the deformation is smaller than in the oxidized compound ($\sigma$ in Table III). The ($NiO_4$) polyhedra lie parallel to the (100) plane, exactly as the (CuO4) polyhedra in $Sr_2CuO_3$ (*12, 13*). The electronic configuration of this type of Ni is not experimentally determined, but one can assume it to be similar to that of Cu(II). The polyhedron around the rare earth is also of interest. It is strongly compressed along the [001] direction in the oxidized phase, giving rise to so anisotropic properties ($\sigma$ in Table III). Removing oxygen makes this polyhe-

dron weakly distorted ($\sigma = 0.11$) in a similar way as in $Sr_2CuO_3$.

The in-plane localization of potentially favourable oxygen vacancy sites in $La_{2-x}Sr_xNiO_y$ may be of importance for understanding the superconducting properties of $La_{2-x}Sr_xCuO_y$. It is well known that $T_c$ passes through a maximum as one increases the Sr content (*24*). Oxygen vacancies are created simultaneously with the introduction of Sr. According to the above discussion, and in agreement with previous determinations by Nguyen *et al.* (*25*), we suppose these to lie preferentially in the *a-b* plane. Obviously, these vacancies are partially filled during air annealing, but one can expect a small amount of remaining oxygen vacancies. These will be detrimental for superconductivity. It may be objected that the oxygen treatment at high pressure used for restoring the stoichiometry to $O_4$ (*24*) should fill these vacancies. This is in fact not absolutely certain as first, interstitial excess oxygen is known to exist in the structure (*26, 27*), and second, from a thermodynamic point of view, interstitial oxygen should always be accompanied by the presence of oxygen vacancies (*28, 29*). We therefore suggest that high oxygen pressure treatment does not necessarily result in a filling of all the oxygen vacancies created by the introduction of strontium. As this effect should be more pronounced for larger Sr level, this could explain the presence of a maximum in $T_c$ as a function of the strontium content.

## Conclusion

Oxygen deficiency in the $La_{2-x}Sr_xNiO_y$ phases can be extended up to a very high level, as proved by the synthesis of the strongly reduced nickelate $LaSrNiO_{3.1}$. Evidence for lowering of the octahedral coordination, V-square-pyramidal and IV-square, are obtained both from crystallographic and local XAS analysis. These new data represent another example of the defect chemistry of oxide-type perovskite. More precisely, the highly ordered distribution of oxygen vacancies along the *b* axis of the orthorhombic cell is highly consistent with the linear clustering oxygen defect model (*30*) which accounts well for oxygen deficiency in other reduced nickelates such as $La_4Ni_4O_{11}$, i.e., $LaNiO_{2.75}$ (*31*).

## References


1. R. Cava, A. Santoro, D. W. Johnson, Jr., and W. W. Rhodes, *Phys. Rev. B* **35,** 6716 (1987).
2. I. D. Brown, submitted for publication.
3. M. Crespin, P. Levitz, and L. Gatineau, *J. Chem. Soc. Faraday Trans. 2* **79,** 1181 (1983); **79,** 1195 (1983).
4. M. Crespin, J. M. Bassat, P. Odier, P. Mouron, and J. Choisnet, *J. Solid State Chem.* **84,** 165 (1990).
5. F. C. Chou, J. H. Cho, L. L. Miller, and D. C. Johnston, *Phys. Rev. B* **42,** 6172 (1990).
6. A Douy and P. Odier, *Mater. Res. Bull.* **249,** 1119 (1989).
7. R. Saez-Puche, J. L. Rodriguez, and F. Fernandez, *Inorg. Chem. Acta* **140,** 151 (1987).
8. J. Rodriguez-Carvajal, M. T. Ferandez-Diaz, and J. L. Martinez, *J. Phys.: Condens. Matt* **3,** 3215 (1991).
9. Y. Takeda, R. Kanno, M. Sakano, O. Yamamoto, M. Takano, Y. Bando, H. Akinaga, K. Takita, and J. B. Goodenough, *Mater. Res. Bull.* **25,** 293 (1990).
10. R. J. Cava, B., Batlogg, T. T. Palstra, J. J. Krajewski, W. F. Peck, Jr., A. Ramirez and L. W. Rupp, Jr., *Phys. Rev. B* **43,** 1229 (1991).
11. G. Demazeau, M. Pouchard, and P. Hagenmuller, *J. Solid. State Chem.* **18,** 159 (1976).
12. M. T. Teske and H. K. Muller-Buschbaum, *Z. Anorg. Allg. Chem.* **371,** 325 (1969).
13. M. T. Weller and D. R. Lines, *J. Solid State Chem.* **82,** 21 (1989).
14. D. M. de Leeuw, C. A. H. A. Mutsaers, C. Langers, H. C. A. Smoorenburg, and B. J. Roommers, *Physica C* **152,** 39 (1988).
15. C. Landron, D. Ruffier, B. Dubois, P. Odier, D. Bonnin, and H. Dexpert, *Phys. Status Solidi A* **121,** 359 (1990).
16. A. G. McKale, B. W. Veal, A. P. Paulikas, S. K. Chan, and G. S. Knapp, *J. Am. Ceram. Soc.* **110,** 3763 (1988).
17. U. von Lehmann and H. K. Muller-Buschbaum, *Z. Anorg. Allg. Chem.* **470,** 59 (1980).
18. J. Choisnet, J. M. Bassat, H. Pilliere, P.

ODIER, AND M. LEBLANC, *Solid State Commun.* **66,** 1245 (1988).
19. D. BAZIN, private communication.
20. M. HIDA, N. WADA, H. MAEDA, H. TERAUCHI, Y. TSU, N. KAMIJO, *Jpn. J. Appl. Phys.* **24,** L3 (1985).
21. T. BEIN, S. J. MCLAIN, G. D. STUCKY, G. WOLERY, D. E. SAYERS, AND K. MOLLER, *J. Phys.* **12,** C8-277 (1986).
22. PH. MONOD, private communication.
23. B. K. TEO, "EXAFS: Basic Principles and Data Analysis," Inorganic Chemistry Concepts Series, Vol. 9, Springer-Verlag, Berlin (1986).
24. J. B. TORRANCE, A. BEZINGE, A. I. NAZZAL, T. C. HUANG, S. S. P. PARKIN, D. T. KEANE, S. J. LAPLACA, P. M. HORN, AND G. A. HELD, *Phys. Rev. B* **40,** 8872 (1989).
25. N. NGUYEN, J. CHOISNET, M. HERVIEU, AND B. RAVEAU, *J. Solid State Chem.* **39,** 120 (1981).
26. J. D. JORGENSEN, B. DABROWSKI, S. PEI, D. B. RICHARDS, AND D. G. HINKS, *Phys. Rev. B* **40,** 2187, (1989).
27. M. Y. SU, E. A. COOPER, C. E. ELSBERND, AND T. O. MASON, *J. Am. Ceram. Soc.* **73,** 3453 (1990).
28. F. A. KROGER, "The Chemistry of Imperfect Crystals," North-Holland, Amsterdam (1974).
29. N. L. ALLEN AND W. C. MACKRODT, *J. Am. Ceram. Soc.* **73,** 3175 (1990).
30. J. A. M. VAN ROOSMALEN AND E. H. P. CORFUNKE, *J. Solid State Chem.* **93,** 212 (1991).
31. J. M. GONZALES-CALBET, M. SAYAGUÈS, AND M. VALLET-REGI, *Solid State Ionics* **32/33,** 721 (1989).